RSC Advances

ROYAL SOCIETY OF CHEMISTRY

www.rsc.org/advances

RSC Advances

ARTICLE

A Sensitive Immobilization-Free Electrochemical Assay for T4PNK Activity Based on Exonuclease III-Assisted Recycling

Received 00th January 20xx,
Accepted 00th January 20xx

DOI: 10.1039/x0xx00000x

www.rsc.org/

Yonghong Wang,[a,b] Yaohui Wu, *,[a] Yuanqing Wang,[a] Bo Zhou [a], Shun Wu [a]

Coupling properties of T4 polynucleotide kinase (T4PNK) catalyzing the transfer of ATP γ-phosphate residue to 5′-hydroxyl termini of nucleic acids, with lambda exonuclease (λ-exo), a highly processive 5′-3′ exonuclease, digesting the 5′-phosphorylated strand of a double DNA to produce single-strand DNA and mononucleotides, this work develops a highly sensitive immobilization-free electrochemical method for detection of T4PNK activity based on λ-exo and exonuclease III-assisted signal amplification. Upon the reaction of T4PNK and λ-exo on substrate-DNA, single-stranded DNA segments (released-ssDNA) are dissociated to hybridize with methylene blue-labeled hairpin probe (MB-DNA) and then the digestion of MB-DNA from the blunt 3 terminus by exonuclease III is activated, resulting in the release of MB-labeled mononucleotides and the complementary DNA segment, followed by the latter hybridizing with another MB-DNA to initiate the cycling process. With smaller size and less negative charge, the MB-labeled mononucleotide thus diffuses facilely to the negatively charged indium tin oxide (ITO) electrode, actuating an amplified electrochemical signal, and the detection limit of the proposed assay can reach as low as 0.005 U/ml. Additionally, this assay can avoid the sophisticated probe immobilization processes. Therefore, this strategy exhibits merits of high sensitivity, simplicity, immobilization-free for electrochemical assay of T4PNK activity, which is consequently believed to bear considerable potential as a detection platform for related researches.

Introduction

Originally discovered in protein extracts of Escherichia coli bacteria infected with T-even phage [1] and acknowledged to be one of the most frequently used enzymes in molecular biology, T4 polynucleotide kinase (PNK) functions as an indispensable epigenetic event that manages cell function by altering gene expression [2]. Briefly, it is capable of phosphorylating DNA at 5′-OH termini through catalyzing the transfer of the γ-phosphate residue of ATP to nucleic acids and oligonucleotides, and also acting as a DNA 3′-phosphatase, consequently playing a vital role in assay of DNA adducts, oligonucleotides, nucleic acid metabolism and repair of DNA lesions [3]. Furthermore, it is performed by some reports that aberrant PNK activity is closely related to critical human disorders such as Bloom syndrome, Werner syndrome, and Rothmund-Thomson syndrome [4]. Additionally, PNK inhibition is much likely to enhance the sensitivity of human tumors to γ-radiation, also representing a prosperous means of improving efficacy of existing cancer treatments [5]. In this case, it is of tremendous value to develop accordingly a sensitive and simple assay for PNK activity and its potential inhibitor as well.

Conventionally, several approaches were described for the detection of phosphorylation and the activity assay of DNA kinase, radical isotope ^{32}P-labeling, polyacylamide gel electrophoresis (PAGE), autoradiography and fluorescence included [6]. Nevertheless, they were somewhat time-consuming, laborious, radio labeling or complex. Recently, to conquer these drawbacks, a great variety of strategies for sensitive detection of PNK activity assays have been developed, including fluorescence assays [7], colorimetric assays [8] and electrochemical assays [9]. For instance, Song et al. combined β-cyclodextrin polymer-based fluorescence enhancement of pyrene with exonuclease reaction for sensitive T4PNK activity detection [10]. Hou et al. developed a fluorescence assay for the detection of PNK activity based on the coupled λ-exo cleavage reaction and catalytic assembly of bimolecular beacons [11]. Lian et al. realized the detection of PNK activity by means of a DNA phosphorylation-accelerated λ-exo cleavage reaction coupled with cationic conjugated polymer-mediated fluorescence resonance energy transfer [12]. In spite of remarkable advances toward the DNA phosphorylation detection made by these previous protocols, further promotion of the analytic performances, involving convenience, fast response and high sensitivity in particular, was not yet to satisfy the increasing needs for biological research, clinic diagnostics, and drug discovery.

Compared with methods as radioactive, fluorescence and PAGE systems, electrochemical biosensors have otherwise attracted considerable interest in phosphorylation assay because

[a] College of Life Science and technology, Central South University of Forestry and Technology, 410004, Changsha, China. E-mail: bionano@163.com
[b] State Key Laboratory of Chemo/Biosensing and Chemometrics, College of Biology, College of Chemistry and Chemical Engineering, Hunan University, 410082, Changsha, China.

of their simplicity, rapid response, cost-effective, sensitive and potential ability for real-time and on-site analysis [13]. In the past decade, a surging number of biosensors accordingly have been designed for the detection of kinase activity by investigating the current and charge responses of redox probes conjugated during the phosphorylation processes. Besides, to further improve the sensitivity of the biosensors, several methods have been developed through exploiting signal amplification strategies [14], among which target recycling is of high thought-put, allowing a single target molecule to interact with multiple nucleic acid-based signaling probes and thus offering an intriguing alternative to achieve signal amplification. In as-proposed approach, after triggering the selective displacement or digestion of the signaling probe, the target-probe hybridization sequently releases the intact DNA target to actuate the displacement or digestion of other signaling probes, thus leading to multiple signaling events and gaining signal amplification. Previously and successfully, these signal amplification strategies have been developed based on fluorescence and electrochemical measurement, issuing in impressive detection sensitivity [15]. Being worthy of mentioning, in contrast to traditional immobilization protocols, the immobilization-free process owns merits of reproducible measurements performed by simple electrode washing step. Moreover, it is superior in efficiency to the hybridization of the target to the electrode-bound probe since it can avoid effectively steric hindrance. Hence in view of both, namely combining target recycling with the immobilization-free electrochemical detection method is much likely to be a robust and promising strategy enjoying advantage of improved sensitivity and no longer requiring for extra operation process and instrumentation.

In this study, we demonstrated an immobilization-free electrochemical methylene blue-labeled hairpin probe (MB-DNA)-based method for detection of enzyme activity with signal amplification by exonuclease III-assisted recycling which is believed to be reported for the first time using electrochemical assay method to detect T4PNK activity. The principle is on the basis of differential diffusivity between electroactive species-labeled oligonucleotides and electroactive species-labeled mononucleotides on a negatively charged electrode surface due to the enzymatic cleavage activity of exonuclease III. In this way, not only does this strategy provide a novel, immobilization-free, simple and sensitive platform for DNA polynucleotide kinase-concerned biological processes evolution, yet also hold a tremendous potential to apply in assay for other essential enzymes and biomolecular diagnosis.

Experimental

Materials and Chemicals

T4 polynucleotide kinase (T4PNK), Lambda exonuclease (λ-exo), adenosine diphosphate (ADP) and adenosine triphosphate (ATP) were purchased from Invitrogen Technology (Shanghai, China). We designed the substrate-DNA and methylene blue-labeled DNA (MB-DNA) and were synthesized by Sangon Biotech Co., Ltd. (Shanghai, China) and the sequences were listed in Table 1. All other chemicals used were of analytical reagent grade and used without further purification. All aqueous solutions were prepared and diluted using ultrapure water (specific resistance >18.2 MΩ·cm) from the Millipore Milli-Q water system (Millipore, Bedford, MA).

Table 1 Sequences of oligonucleotides used in the experiments.

Oligonucleotides	Sequences
Substrate-DNA	5'-**GATTTTTCCTTCTCG**GAACAAAAGGAA GATACGT A**CGAGAAGGAAAAATC**-3'
MB-DNA	5'-**AGGAAGA**CGTACGTA**TCTTCCT**TTTGT T -**MB**-C-3'

Instruments

A CHI660E electrochemical workstation (Beijing Chinese Science Days Technology Co., Ltd., Beijing, China) was chosen for differential pulse voltammetry (DPV). The electrochemical workstations had a three-electrode mode comprising an indium tin oxide (ITO) electrode, a platinum counter electrode and an Ag/AgCl reference electrode. All the potentials in this work were with respect to Ag/AgCl electrode. Before each electrochemical measurement, the ITO electrodes were sequentially sonicated in an Alconox cleaning detergent, acetone, ethanol and water lasting for 15 min each. After these clean procedures, a negatively charged surface could be obtained [15e].

T4PNK-Catalyzed Phosphorylation

All DNA samples were prepared in 10 mM Tris-HCl buffer (pH 7.4, 10 mM $MgCl_2$). The concentration of the substrate-DNA stock solution was 10 μM, and the concentration of the MB-DNA stock solutions was 10 μ M. Prior to T4PNK enzyme reaction, all DNA samples were pretreated with the following procedure respectively: heated to 90 ℃ and incubated for 5 min, and then cooled slowly to 37 ℃ and incubated for 1 h. The obtained DNA solutions were stored at 4 ℃ for further use.

In a typical phosphorylation and cleavage assay, consisting of 10 mM Tris-HCl, 100 nM substrate-DNA, 10 mM $MgCl_2$, 1.0 mM ATP, 10 units λ-exo and a certain amount of T4PNK, the 200 μL enzyme reaction buffer could introduce phosphorylation site at the 5'-hydroxyl termini and cause the formation of 5'-phosphoryl termini product that could be recognized by λ-exo. The resulting solution was kept at 37 ℃ for a certain period of time before the electrochemical measurements.

Assay Optimization

For purpose of fulfilling the best sensing effect, several important conditions were optimized respectively, the λ-exo concentration, ATP concentration, MB-DNA concentration and reaction time included. The λ-exo concentration range was 1.0-15.0 units, ATP concentration range 0.1-5.0 mM, MB-DNA concentration 0.1-10 μM, and the reaction time range 0 to 60 min. Equal volume of T4PNK storage buffer was added in each enzyme reaction mixture respectively.

Exonuclease III-assisted T4PNK Activity Detection

A volume of 200 μL of Tris-HCl buffer containing 5 μM MB-DNA, 10 units of exonuclease III and the released-ssDNA produced by T4PNK-catalyzed phosphorylation was incubated at 37 ℃ for a certain period of time. Then, for each DPV scanning, 20 μL of the mixture solution was pipetted onto the ITO working electrodes. Before the experiments, the electrolyte buffer was washed by ultrapure water and then thoroughly purged with nitrogen gas. And DPV measurements were conducted in 10 mM Tris-HCl (pH 7.4) containing 50 mM KCl by scanning the potential from -0.2 to 0.5 V, with the modulation amplitude of 25 mV and the scan rate of 100 mV/s. All the measurements were repeated for at least five times.

Influence of Inhibitors on T4PNK Activity

In order to further evaluate the inhibitors screening ability of the proposed assay, two known inhibitors of T4PNK, namely ADP and $(NH_4)_2SO_4$ with different concentrations were added in the reaction buffer, respectively. Then 1.0 mM ATP, 10 units of λ-exo, and 10 units of T4PNK were added before the reaction solution was kept at 37 ℃ for 30 min. The detection processes were recorded using the aforementioned procedure.

Results and Discussion

Design Strategy of T4PNK Activity Detection

As shown in Figure 1, the principle for strategy was that T4PNK could catalyze the transfer of the γ-phosphate residue of ATP to 5'-hydroxyl termini of nucleic acids, and λ-exo was a highly processive 5'-3' exonuclease capable of digesting the 5'-phosphorylated strand of a double DNA to generate single-strand DNA and mononucleotides. In the absence of T4PNK, substrate-DNA could maintain the stem-loop structure due to the binding of the complementary sequences at the ends, in which case released-ssDNA could not be produced and because of the electrostatic repulsion, MB-DNA could not yet get close to the negative ITO electrode. Therefore, the electrode exhibited a negligible electrochemical signal. Whereas in the presence of T4PNK and λ-exo, T4PNK catalyzed the phosphorylation reaction toward the hydroxyl group at the 5'-termini of the substrate-DNA to yield the 5'-phosphorylated substrate-DNA, which could be immediately cleaved by λ-exo, resulting in the released-ssDNA. Furthermore, the amount of released-ssDNA was positively related to the activity of T4PNK. Then the released-ssDNA hybridized with MB-DNA whose stem-loop structure was opened, forming a double-stranded DNA with a receded 3′ terminus, which subsequently initiated the digestion by exonuclease III to degrade the MB-DNA from the 3′ terminus and liberate the electroactive species. In this way, the electrochemical signal could be observed. It should be noted that exonuclease III could recognize and cleave from the 3' end of a duplex DNA with a blunt or receded 3' terminus, and a duplex DNA with a protruded 3'-terminus was not a substrate for exonuclease III. Since the 3' terminus of the released-ssDNA in the double-stranded DNA was not fully hybridized to its complementary stand, the released-ssDNA would not be digested by exonuclease III. So the released-ssDNA then could hybridize with MB-DNA and enter a new cycle, therefore amplifying the signal and dramatically increasing the detection sensitivity with an extremely lo amount of released-ssDNA. Thus, sensitive electrochemical detection of T4PNK based on the exonuclease III-aided signal amplification was fulfilled.

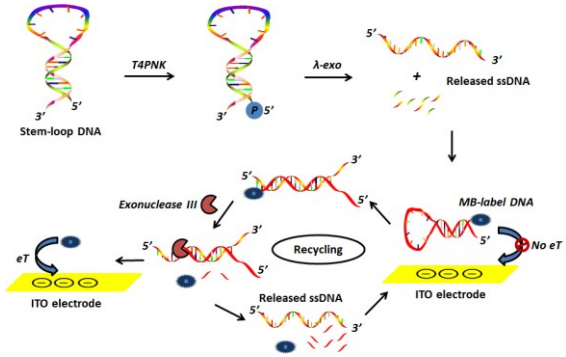

Figure 1. Schematic illustration for T4PNK activity detection based on λ-exo cleavage reaction and exonuclease III-assisted signal amplification.

Feasibility of Detection of T4 PNK Activity

To verify the feasibility, agarose gel electrophoresis experiment were employed. The DNA phosphorylation-induced digestion of substrate-DNA by λ-exo was primary in this strategy, which thus was examined by gel electrophoresis. As shown in Figure 2A, in the absence of T4PNK or λ-exo, an obvious band was observed, indicating no substrate-DNA digestion. When T4PNK and λ-exo both presented, no obvious band was observed, indicating a high efficiency of phosphorylation induced digestion of substrate-DNA by λ-exo in the presence of T4PNK. Additionally, after the MB-DNA and released-DNA incubated with exonuclease III, the ban was disappeared. The results were identical to what as expected.

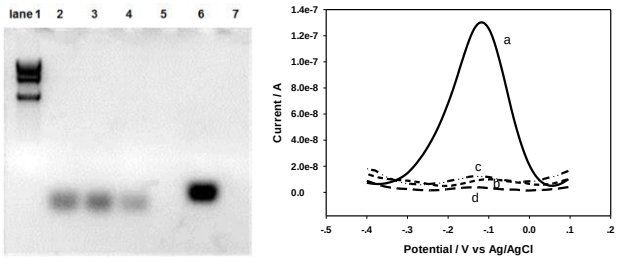

(A) (B)

Figure 2. (A) Agarose (2%) gel electrophoresis image. Lane 1: marker; lane 2: substrate-DNA, lane 3: substrate-DNA+T4PNK; lane 4: substrate-DNA+λ-exo; lane 5: substrate-DNA+T4PNK+λ-exo; lane 6: released-DNA+MB-DNA; lane 7: released-DNA+MB-DNA+exonuclease III; (B) DPV scans of reaction mixtures in response to different controls. a) T4PNK + λ-exo + exonuclease III, all the three enzymes existing in the reaction mixture; b) in the absence of T4PNK in the reaction mixture; c) in the absence of λ-exo in the reaction mixture; d) in the absence of Exonuclea III in the reaction mixture.

DPV measurements were further applied to prove the proposed strategy. As shown in Figure 2B, a significant detectable current signal of methylene blue was observed wh

all the three enzymes of T4PNK, λ-exo, and exonuclease III were present (curve a). Whereas in the absence of T4PNK (curve b), λ-exo (curve c), or exonuclease III (curve d), no obvious current response was shown owing to the electrostatical repulsion between the negatively charged ITO electrode and the negative MB-DNA backbones. In this way, a single released-ssDNA was able to trigger the digestion of multiple MB-DNA into the more diffusive electrochemical indicator (MB), which thereby generated an amplified electrochemical signal. Therefore, this result demonstrated the feasibility of this method for the assay of T4PNK activity.

Optimization of Assay Conditions

The time of phosphorylation was a vital parameter in optimizing the signal gain of electrochemical strategy. It was found that the currents response of the electrochemical assay was strongly affected by the T4PNK incubation time. As shown in Figure 3A, with the increase of the phosphorylation time, the currents response increased and tended to the relative maximum current signal at 30 min. Nevertheless, with further increase in the phosphorylation time, the current response otherwise did not increase accordingly, which suggested that the phosphorylation reaction was done not more than 30 min. Thus, 30 min in following experiments was chosen as the appropriate time.

ATP played an important role in the phosphorylation process, whose influence of concentration thus was examined, and the results were shown in Figure 3B. It could be seen that with the ATP concentration increasing, the higher current responses of the DNA phosphorylation were observed. While the concentration of ATP was >1.0 mM, a slight decrease was shown. Caused by higher concentrations of ATP during the phosphorylation process, this slight inhibition effect was possibly attributed to a competitive binding reaction between the DNA and ATP. As a result, when the concentration of ATP was relatively high, the binding site of T4PNK was partially blocked. Therefore, 1.0 mM was employed as the optimal ATP concentration to obtain a high sensitivity.

The released-ssDNA from the hairpin substrate DNA could affect the hybridization with the MB-DNA probe, eventually determining the detection sensitivity. In this point of view, different λ-exo concentrations were evaluated that could liberate released-ssDNA upon phosphorylation by T4PNK and digestion by λ-exo. The current intensity was found to increase with the amount of λ-exo and almost reached the saturation value at an amount of 10 units of λ-exo (Figure 3C). Thus, 10 U λ-exo was selected for following experiments.

Identically, the initial amount of MB-DNA also served as an indispensable substrate in the performance of the assay. Provided the initial concentration of MB-DNA was too high, most MB-DNA would overcome the electrostatic repulsion and diffuse to the electrode surface, issuing in a strong background signal. From the other respect, if the initial concentration of MB-DNA was too low, a small electrochemical signal would still be observed though when all the MBs were digested by exonuclease III, making it difficult to distinguish the signal from noises. Thus, concentration of MB-DNA ranging from 0.1 to 10 μM was studied and the condition of 5 μM MB-DNA was fixed due to its best signal-to-noise ratio (Figure 3D). Therefore, the concentration of MB-DNA was optimized at 5 μM in all the following experiments.

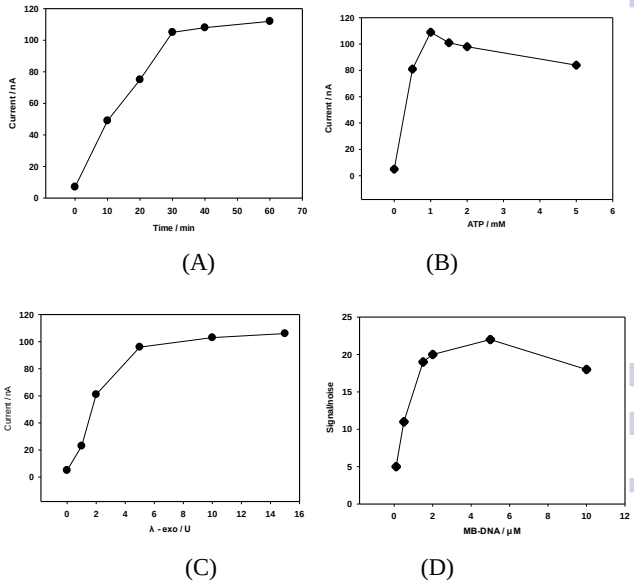

Figure 3. A) The curves of the different incubation time for phosphorylation at 37 ℃ (0-60 min); B) The curves of different ATP concentration (0.1-5 mM); C) The curves of different λ-exo concentration (0-15 U); D) The signal-to-noise ratio of different MB-DNA concentration (0.1-10 μM).

Electrochemical Assay of T4PNK Activity

Using this fabricated electrochemical platform, a series of different concentrations of T4PNK (from 0.005 to 20 UmL^{-1}) were assayed to demonstrate the ability of the detection to sensitively quantify T4PNK activity under the optimum experimental conditions. As shown in Figure 4A, it was performed that with an increase in the concentration of T4PNK varied from 0.005 to 20 UmL^{-1}, the DPV signal increased gradually. The corresponding results were shown in Figure 4B which displayed the relationship between currents signal and the T4PNK concentration, and in Figure 4B inset, a relatively good linearity was in the range from 0.005 U/mL to 1.0 U/mL. The correlation equation could be described as $I= 5.28\times10^{-7}X +1.65\times10^{-8}$ with the correlation coefficient $R^2= 0.9618$, where I was current intensity, and X was T4PNK concentration. The direct detection limit of the method was 0.005 U/mL. It was demonstrated through the result that exonuclease III-aided signal amplification strategy could remarkably upgrade the detection sensitivity and it was facile to observe the signal even when T4PNK concentration was at as low as 0.005 U/mL. The developed method achieved comparable or even better sensitivity against some other signal amplification strategy listed in Table 2. In previous methods employing electrode-bound MB-DNA, compromised by the hindrance effect of the electrode surface and the limited conformational freedom of the bound MB-DNA, the high selectivity with hairpin structure was often restrained. Different from traditional MB-DNA based electrochemical biosensors in which the MBs should be immobilized on the electrode surface and the reaction of

sequence recognition and hybridization, the immobilization-free process in this method bore merits of reproducible measurements performed by simple electrode washing step. Moreover, it was more efficient than hybridization of the ssDNA to the electrode-bound probe because it could avoid steric hindrance to a great extent.

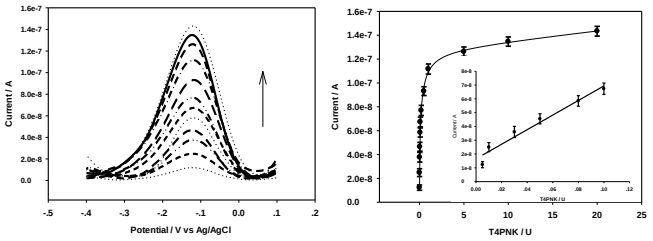

(A) (B)

Figure 4. A) DPV curves response to different concentrations of T4PNK. The different concentrations of T4PNK at 0.005, 0.01, 0.03, 0.05, 0.08, 0.10, 0.20, 0.50, 1.0, 5.0, 10.0 and 20.0 U/mL respectively; B) Concentration curves for T4PNK. Linear relationship between the current and the concentrations of the T4PNK from 0.005 to 0.1 U/ml showed in inset.

Table 2. Comparison of analytical performance for T4PNK activity detection by different reported methods.

Strategy	Technique	LOD (U/ml)	Linear range (U/ml)	Reference
β-cyclodextrin polymer enhanced	fluorescence	0.02	0-0.25	10
Coupled λ-exo and catalytic assembly of bimolecular beacons	fluorescence	0.001	0.001-0.1	11
λ-exo cleavage-induced DNAzyme releasing strategy	fluorescence	0.005	0.005-0.2	14a
Coupled λ-exo and exonuclease III recycling	fluorescence	0.01	0.01-1	16a
TiO_2 nanotubes and Au nanoparticles	electrochemical	0.003	0.01-10	9a
Ferrocene-functionalized SWCNT	electrochemical	0.01	0.01-0.1	9b
Dual-signaling amplification coupled with exonuclease reaction	electrochemical	0.02	0.05-10	16b
Streptavidin-gold nanoparticles and enzymatic amplification	electrochemical	0.01	0.01-5	16c
Coupled exonuclease and graphene oxide platform	electrochemical	0.05	0.05-10	14d
Based on exonuclease III-assisted recycling	electrochemical	0.005	0.005-1.0	This work

To evaluate the feasibility of the proposed assay, we have further investigated its analytical performance for T4PNK detection in biological samples. The samples were prepared by adding T4PNK in 50% cell lysates contained reaction buffer, which thus were employed to simulate the intracellular environment during the test procedure. As shown in Figure 5, in a reaction system containing cell lysates, a gradual increase current signal was observed as the concentration of T4PNK increases. In this case, the result was in good agreement with those in pure reaction buffer without cell lysates, suggesting that this method could be applicable for T4PNK detection in biological samples.

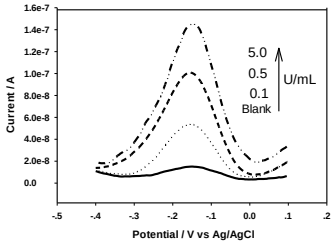

Figure 5. DPV curves response of this system for various activity of T4PNK in 50% cell lysate.

Evaluation of T4PNK Activity Inhibition

In order to exploit the possible application in the inhibition assay, the validity of the developed method to evaluate the inhibitors of T4PNK was proved by using ADP and ammonium sulfate as model inhibitors. Both ADP and ammonium sulfate, as shown in Figure 6, remarkably inhibited phosphorylation process in a dose-dependent manner. Then, the half-maximal inhibitory concentration values were determined for the T4PNK inhibitors to further demonstrate the utility of this assay used in a quantitative inhibition assay. The addition of 15 mM $(NH_4)_2SO_4$ or 1.5 mM ADP could inhibit phosphorylation by approximately 50%. The results manifested that this approach could exert various effects on phosphorylation quickly and simply.

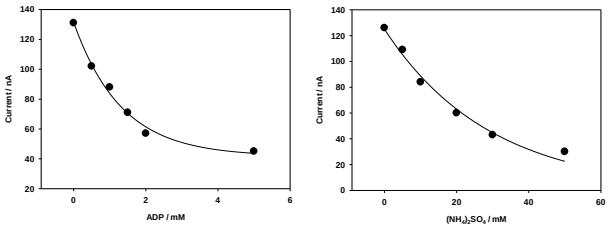

(A) (B)

Figure 6. The effect of different concentrations of T4PNK inhibitors. A) Different concentrations of ADP (0-5 mM); B) Different concentrations of $(NH_4)_2SO_4$ (0-50 mM). The assay was carried out in the reaction buffer solution containing 10 U T4PNK, 1.0 mM ATP and 10 U λ-exo.

Conclusions

In this paper, we described an electrochemical-sensing platform for immobilization-free, signal-on and highly sensitive detection of the activity and inhibition of T4PNK based on an exonuclease III-assisted recycling strategy. Since the step of DNA immobilization was eliminated, the target detection would not demand any labour or time consumption. Taking advantage of the unique strategy of signal amplification, the detection limit could reach extreme low as 0.005 U/mL. Besides, this assay could be utilized in screening inhibitors of T4PNK. In terms of its appealing analytical characteristics, this sensing strategy possibly was endorsed with major applications in biomedical research. Provided further developed to an

electrochemical microarray assay, it would enjoy an infinitely promising employment in researching on the interactions between proteins and nucleic acids.

Acknowledgements

This work was supported in part by the National Natural Science Foundation of China (21305164), State Key Laboratory of Chemo/Biosensing and Chemometrics, Hunan University (2013019).

Notes and references

1 C.C. Richards, Proc. Natl. Acad. Sci. U.S.A. 1965, **54**, 158.
2 C.J. Whitehouse, R.M. Taylor, A. Thistlethwaite, H. Zhang, F. Karimi-Busheri, D.D. Lasko, M. Weinfeld, K.W. Caldecott, Cell. 2001, **104**, 107.
3 (a) D.H. Phillips, V.M. Arlt, Nat. Protoc. 2007, **2**, 2772; (b) A. Rasouli-Nia, F. Karimi-Busheri, M. Weinfeld, Proc. Natl. Acad. Sci. U.S.A. 2004, **101**, 6905; (c) M. El-Atifi, I. Dupre, B. Rostaing, A.L. Benabid, F. Berger, Biotechniques. 2003, **35**, 262; (d) C. Ma, X. Yang, K. Wang, Z. Tang, W. Li, W. Tan, X. Lv, Anal. Biochem. 2008, **372**, 131; (e) C. Frauendorf, F. Hausch, I. Rohl, A. Lichte, S. Vonhoff, S. Klussmann, Nucleic Acids Res. 2003, **31**, e34; (f) F. Karimi-Busheri, A. Rasouli-Nia, J. Allalunis-Turner, M. Weinfeld, Cancer Res. 2007, **67**, 6619.
4 S. Sharma, K.M. Doherty, R.M. Brosh, J. Biochem. 2006, **398**, 319.
5 (a) G.K. Freschauf, F. Karimi-Busheri, A. Ulaczyk-Lesanko, T.R. Mereniuk, A. Ahrens, J.M. Koshy, A. Rasouli-Nia, P. Pasarj, C.F. Holmes, F. Rininsland, D.G. Hall, M. Weinfeld, Cancer Res. 2009, **69**, 7739; (b) S.L. Allinson, Future. Oncol. 2010, **6**, 1031.
6 (a) L.K. Wang, S. Shuman, J. Biol. Chem. 2001, **276**, 26868; (b) C. Chappell, L.A. Hanakahi, F. Karimi-Busheri, M. Weinfeld, S.C. West, EMBO J. 2002, **21**, 2827; (c) M. Meijer, F. Karimi-Busher, T.Y. Huang, M. Weinfeld, D. Young, J. Biol. Chem. 2002, **277**, 4050.
7 (a) C. Ma, H. Fang, K. Wang, K. Xia, H. Chen, W. Zeng, Anal. Biochem. 2013, **443**, 166; (b) F. Zhou, G. Wang, D. Shi, Y. Sun, L. Sha, Y. Qiu, X, Zhang, Analyst. 2015, **140**, 5650; (c) M. Tao, Z. Shi, R. Cheng, J. Zhang, B. Li, Y. Jin, Anal. Biochem. 2015, **485**, 18;
8 (a) H-X. Jiang, D-M. Kong, H-X. Shen, Biosens. Bioelectron. 2014, **55**, 133; (b) C. Jiang, C.Y. Yan, J.H. Jiang, R.Q. Yu, Anal. Chim. Acta, 2013, **766**, 88; (c) Z. Wang, R. Lévy, D.G. Fernig, M. Brust, J. Am. Chem. Soc. 2006, **128**, 2214.
9 (a) G. Wang, X. He, G. Xu, L. Chen, Y. Zhu, X. Zhang, L. Wang, Biosens. Bioelectron. 2013, **43**, 125; (b) Y. Wang, X. He, K. Wang, X. Ni, J. Su, Z. Chen, Biosens. Bioelectron. 2012, **32**, 213; (c) S. Liu, T. Liu, L. Wang. Chem. Commun., 2015, **51**, 176.
10 C. Song, X. Yang, K. Wang, Q. Wang, J. Liu, J. Huang, L. He, P. Liu, Z. Qing, W. Liu, Chem. Commun. 2015, **51**, 1815.
11 T. Hou, X. Wang, X. Liu, T. Lu, S. Liu, F. Li, Anal. Chem. 2014, **86**, 884.
12 S. Lian, C. Liu, X. Zhang, H. Wang, Z. Li, Biosens. Bioelectron. 2015, **66**, 316.
13 D. Grieshaber, R. MacKenzie, J. Vörös, E. Reimhult, Sensors. 2008, **8**, 1400.
14 (a) S.F. Liu, J.J. Ming, Y. Lin, C.F. Wang, T. Liu, C.B. Cheng, F. Li, Sens. Actuators B: Chem. 2014, **192**, 157; (b) L. Zhang, T. Hou, H. Li, F. Li, Analyst. 2015, **140**, 4030; (c) Y. Wang, Y. Li, H. Ma, X. Ren, W. Cao, T. Yan, Q. Wei, RSC Adv. 2015, **5**, 31262; (d) L. Lin, Y. Liu, X. Zhao, J. Li, Anal. Chem. 2011, **83**, 8396.
15 (a) X. Wu, Y. Chai, P. Zhang, R. Yuan, ACS Appl. Mater. Interfaces. 2015, **7**, 713; (b) S. Liu, Y. Wang, C. Zhang, Y. Lin, F. Li, Chem. Commun. 2013, **49**, 2335; (c) J. Su, H. Zhang, B. Jiang, H. Zheng, Y. Chai, R. Yuan, Y. Xiang, Biosens. Bioelectron. 2011, **29**, 184; (d) Q. Xu, A. Cao, L. Zhang, C. Zhang, Anal. Chem. 2012, **84**, 10845; (e) F. Xuan, X. Luo, I-M. Hsing, Anal. Chem. 2012, **84**, 5216.
16 (a) Z-M. Zhu, R-Q. Yu, X. Chu. Anal. Methods-UK, 2014, **6**, 6009; (b) Y. Peng, J. Jiang, R. Yu. RSC Adv. 2013, **3**, 18128; (c) T. Hou, X. Wang, X. Liu, C. Pan, F. Li, Sensor Actuat B-Chem. 2014, **202**, 588.